



Acuren Group Inc.
7450 - 18th Street
Edmonton, AB, Canada T6P 1N8
Phone: (780) 440-2131
Fax: (780) 440-1167

**Materials Engineering & Testing
a Rockwood Company**

May 19, 2011

Our Project No.: 206-11-05-0059227

Plains Midstream Canada
1400 607 8th Avenue SW
Calgary, AB
T2P 0A7

Attention: Mr. Minh Ho

Dear Sir:

SUBJECT: EXAMINATION OF RAINBOW PIPELINE FAILURE

Please find enclosed the above-named report. We trust you will find it satisfactory, and we appreciate the opportunity to be of service to Plains Midstream Canada. At Acuren, we remain committed to providing you with world-class integrity management solutions.

Should you require any additional information, please do not hesitate to contact the undersigned at (780) 490-2432 or by e-mail at thamre@acuren.com

Please note that unless we are notified in writing, samples from this investigation will be disposed of after 60 days.

Sincerely,

E.C. (Ted) Hamre, Ph.D., P. Eng.
Engineering Technical Leader

Enc



ISO 9001:2000



Acuren Group Inc.

7450 - 18th Street
Edmonton, AB, Canada T6P 1N8

Phone: (780) 440-2131
Fax: (780) 440-1167

**Materials Engineering & Testing
a Rockwood Company**

EXAMINATION OF RAINBOW PIPELINE FAILURE

Prepared for

**Mr. Minh Ho
Plains Midstream Canada**

Prepared by

E.C. (Ted) Hamre, Ph.D., P. Eng.
Engineering Technical Leader

Reviewed by

Ken Magee, M.A.Sc., P. Eng.
Senior Metallurgical Engineer

May 19, 2011

Acuren Project No.: 206-11-05-0059227



ISO 9001:2000

TABLE OF CONTENTS

| | |
|--|------------|
| PREFACE | III |
| 1.0 INTRODUCTION | 1 |
| 2.0 INVESTIGATION | 3 |
| 2.1 VISUAL EXAMINATION | 3 |
| 2.2 SCANNING ELECTRON MICROSCOPY | 12 |
| 2.3 NONDESTRUCTIVE INSPECTION | 19 |
| 2.4 METALLOGRAPHY | 25 |
| 2.5 MECHANICAL TESTING | 32 |
| 2.5.1 HARDNESS TESTING | 32 |
| 2.5.2 TENSILE TESTING | 35 |
| 2.5.3 CHARPY IMPACT TESTING | 36 |
| 2.6 CHEMICAL ANALYSIS | 39 |
| 3.0 DISCUSSION | 40 |
| 4.0 CONCLUSIONS | 44 |

LIST OF FIGURES

| | | |
|-----------|--|----|
| FIGURE 1 | LEAKING PIPE SECTION AS RECEIVED | 2 |
| FIGURE 2 | ADJACENT SLEEVE SECTION AS RECEIVED | 2 |
| FIGURE 3 | INITIAL APPEARANCE OF BROKEN PIPE | 4 |
| FIGURE 4 | CRACK PATH FROM BOTTOM OF PIPE TO 2:00 | 4 |
| FIGURE 5 | CRACK PATH FROM BOTTOM OF PIPE TO 10:00 | 5 |
| FIGURE 6 | EXTENT OF OPENING AT BOTTOM OF PIPE | 5 |
| FIGURE 7 | OFFSET OF FRACTURE AT 9:00 | 6 |
| FIGURE 8 | OFFSET OF FRACTURE AT 3:00 | 6 |
| FIGURE 9 | APPEARANCE OF WELD AT BOTTOM OF PIPE | 7 |
| FIGURE 10 | WELD "BUTTON" AT BOTTOM | 7 |
| FIGURE 11 | WELD "BUTTON" | 8 |
| FIGURE 12 | TYPICAL WEAVE PATTERN USED FOR FILLET WELD | 8 |
| FIGURE 13 | WELD APPEARANCE AT 4:30 | 9 |
| FIGURE 14 | WELD APPEARANCE NEAR TOP OF PIPE | 9 |
| FIGURE 15 | PRE-EXISTING CRACK AT FRACTURE ORIGIN | 10 |
| FIGURE 16 | CHEVRON PATTERN ON BRITTLE CRACK POINTING TO FRACTURE ORIGIN AT PRE-EXISTING FEATURE | 10 |
| FIGURE 17 | CHEVRON PATTERN ON BRITTLE CRACK POINTING TO FRACTURE ORIGIN (OPPOSITE SIDE) | 11 |
| FIGURE 18 | INITIAL APPEARANCE OF PRE-EXISTING CRACK SURFACE | 13 |
| FIGURE 19 | CRACK TIP REGION SHOWING EXTENT OF PRE-EXISTING CRACK AND FINAL RUPTURE | 14 |
| FIGURE 20 | SCALE TO TIP OF PRE-EXISTING CRACK | 14 |
| FIGURE 21 | EDX SPECTRUM OF SCALE | 15 |
| FIGURE 22 | PRE-EXISTING CRACK APPEARANCE AFTER 30 SECONDS CLEANING | 15 |
| FIGURE 23 | INTERGRANULAR CRACKING IN HEAT AFFECTED ZONE | 16 |
| FIGURE 24 | CRACK TIP REGION SHOWING ABSENCE OF PROGRESSIVE CRACK GROWTH | 16 |
| FIGURE 25 | CRACK TIP REGION SHOWING ABSENCE OF PROGRESSIVE CRACK GROWTH | 17 |
| FIGURE 26 | FRACTURE SURFACE APPEARANCE AT INSIDE OF PIPE | 17 |
| FIGURE 27 | BRITTLE CLEAVAGE FRACTURE APPEARANCE | 18 |
| FIGURE 28 | DUCTILE APPEARANCE OF INSIDE LIGAMENT | 18 |



| | | |
|-----------|---|----|
| FIGURE 29 | LINEAR INDICATIONS AT TOE OF FILLET WELD | 20 |
| FIGURE 30 | LINEAR INDICATIONS AT TOE OF FILLET WELD | 20 |
| FIGURE 31 | LINEAR INDICATIONS AT WELD TOE AND AT ARC BURN..... | 21 |
| FIGURE 32 | LINEAR INDICATIONS DETECTED BY BLACK ON WHITE MPI | 21 |
| FIGURE 33 | LINEAR INDICATIONS DETECTED BY BLACK ON WHITE MPI | 22 |
| FIGURE 34 | CRACK INDICATION AT BOTTOM OF WELD (UPSTREAM END OF FAILURE SLEEVE) | 22 |
| FIGURE 35 | CRACK INDICATIONS AT TOE OF WELD (UPSTREAM END OF FAILURE SLEEVE) | 23 |
| FIGURE 36 | CRACK INDICATIONS ADJACENT TO TOE OF WELD (UPSTREAM END OF FAILURE SLEEVE)..... | 23 |
| FIGURE 37 | INDICATIONS OF CRACKING AT TOE OF FILLET WELD (SLEEVE ON JOINT 55 300) | 24 |
| FIGURE 38 | INDICATIONS OF CRACKING AT ARC BURN ADJACENT TO FILLET WELD (SLEEVE ON JOINT 55 300)..... | 24 |
| FIGURE 39 | METALLOGRAPHIC SECTION FROM 6:00 POSITION | 26 |
| FIGURE 40 | CRACK PROFILE AT 6:00 POSITION | 26 |
| FIGURE 41 | FRACTURE PATH THROUGH THE WELD | 27 |
| FIGURE 42 | MARTENSITIC MICROSTRUCTURE OF HEAT AFFECTED ZONE WITH INTERGRANULAR FRACTURE PATH..... | 27 |
| FIGURE 43 | PIPE MICROSTRUCTURE | 28 |
| FIGURE 44 | WELD SECTION AT 2:00 | 28 |
| FIGURE 45 | WELD SECTION AT 10:00 | 29 |
| FIGURE 46 | WELD SECTION AT TOP | 29 |
| FIGURE 47 | LACK OF FUSION AT 10:00..... | 30 |
| FIGURE 48 | SECTION FROM UPSTREAM FILLET WELD AT 6:00 | 30 |
| FIGURE 49 | CRACK AT TOE OF UPSTREAM FILLET WELD | 31 |
| FIGURE 50 | UPSTREAM HAZ MICROSTRUCTURE..... | 31 |
| FIGURE 51 | HARDNESS VALUES (HV 500gf) AT 6:00 | 33 |
| FIGURE 52 | HARDNESS VALUES (HV 500gf) NEAR CRACK ORIGIN..... | 33 |
| FIGURE 53 | CHARPY TRANSITION CURVES..... | 38 |

LIST OF TABLES

| | | |
|---------|---|----|
| TABLE 1 | DOWNSTREAM FILLET WELD HARDNESS RESULTS (HV 500gf)..... | 34 |
| TABLE 2 | UPSTREAM FILLET WELD HARDNESS RESULTS (HV 500gf) | 34 |
| TABLE 3 | TENSILE TEST RESULTS..... | 35 |
| TABLE 4 | CHARPY IMPACT TEST RESULTS – LONGITUDINAL SAMPLES | 36 |
| TABLE 5 | CHARPY IMPACT TEST RESULTS – TRANSVERSE SAMPLES | 37 |
| TABLE 6 | CHEMICAL TEST RESULTS | 39 |



PREFACE

SCOPE OF SERVICES

The agreement of Acuren to perform services extends only to those services specifically provided for in writing. Under no circumstances shall such services extend beyond the performance of the requested inspection of specific equipment provided for in writing and the preparation of reports or similar documents. Any descriptions, statements, comments or expressions made reflect the opinion or observations of the Acuren examiner based solely upon data available at the time, and are not intended, nor can they be construed, as representations or warranties as to the actual circumstances. Acuren does not assume any responsibilities of the owner/operator, and the owner/operator retains complete responsibility for all engineering, repair and use decisions.

STANDARD OF CARE

In performing the services provided, Acuren shall use the degree of care and skill ordinarily exercised under similar circumstances by others performing such services in the same or similar locality. **No other warranty, expressed or implied, is made or intended by Acuren, and all other warranties are expressly disclaimed.** In the event of any breach of this warranty, Acuren's sole and exclusive obligation will be to correct or re-perform the deficient service or, at Acuren's option, to refund the amount paid for the deficient service.

LIMITATIONS OF LIABILITY

Nothing in this agreement shall be construed to mean that Acuren assumes any liability on account of injury to persons or property, including death, except and only to the extent those directly caused by the willful or negligent misconduct of Acuren in the context of performing the requested services. In no event shall Acuren's aggregate liability for any reason, in connection with any claim asserted, exceed the amount paid for the services in question. Acuren shall not be held responsible or liable for any loss, damage or delay caused by accidents, strikes, fires, floods, or other circumstances or causes beyond Acuren's control, including actions taken or not taken by the owner/operator or other third parties. In no event shall Acuren be liable for indirect, incidental, special, punitive, or consequential damages including, without limitation, damages relating to reputation, lost profits, goodwill, downtime, loss of use, business interruption or other economic loss.



1.0 INTRODUCTION

A failure occurred on the Plains Midstream 508 mm diameter Rainbow Pipeline on April 28, 2011. The failure occurred as a circumferential crack on the downstream side of the full encirclement sleeve that was present from 5.39 m to 6.92 m downstream of Girth Weld 55310.

The 508.0 mm diameter, 7.14 mm wall thickness, Grade 359 pipe had been manufactured by Stelco and installed in 1967 with a maximum allowable operating pressure of 7260 kPa. The line transported crude oil continuously with a typical operating pressure of 2250 kPa at a temperature of 2.5 to 10°C. The external coating on the pipe was reported to be Plicoflex primer with PVC-butyl tape. At the time of the failure, the external coating condition was reported to be “fair”. The sleeve adjacent to the fracture had been installed in 1980.

All sleeves in the system had been examined for toe cracks in the period 1989 to 1990. As a result of a November 2007 MFL (magnetic flux leakage) tool run, an integrity dig from approximately 2 m downstream of GW 55310 to 3 m downstream of GW 55320 was performed in April 2010. This inspection detected some localized corrosion up to a maximum depth of 33% of the nominal pipe thickness but no evidence of any cracking was found. It was also reported that a pipe line marker post had been welded to the sleeve at the time of sleeve installation and subsequently removed. Magnetic particle inspection was performed at the location where this post had been removed and no evidence of cracking was found. A further MFL tool run was performed in January 2011 that did identify some corrosion in the area with no indication over 60%. A crack detection tool was run in April 2011 and nothing significant was detected in the area of the failure.

The section of pipe containing the crack along with the adjacent sleeve was removed from the line and submitted to Acuren for investigation into the cause of failure (Figure 1). Additionally, a section of pipe containing a second sleeve that had been located on Joint 55300 (just upstream of the joint that ruptured) was also submitted for examination (Figure 2). The findings of these examinations are as follows.





FIGURE 1 LEAKING PIPE SECTION AS RECEIVED



FIGURE 2 ADJACENT SLEEVE SECTION AS RECEIVED



2.0 INVESTIGATION

2.1 VISUAL EXAMINATION

Preliminary examination of the pipe section prior to any cleaning found the maximum opening of the crack to be located at the six o'clock orientation and to be coincident with the toe of the fillet weld joining the end of the sleeve to the carrier pipe, as shown in Figure 3. After removal of the tape coating in the vicinity of the rupture, it was seen that the fracture ran up the sides of the pipe and slightly away from the fillet weld as shown in Figures 4 and 5. The total length of the crack was measured to be 1105 mm, or 69% of the pipe circumference. The maximum opening of the crack at the six o'clock location was 10.7 mm.

The pipe was cleaned using a solvent for approximately 150 mm upstream and downstream of the rupture. This section of pipe was then removed for more detailed examination. The extent of crack opening at the six o'clock location is shown in Figure 6. It was also noted that the fracture had twisted slightly as illustrated in Figures 7 and 8. Visual examination of the pipe in the vicinity of the rupture found no evidence of any significant corrosion or mechanical damage that would have contributed to the crack initiation.

Examination of the pipe at the six o'clock orientation found that the maximum opening was associated with a small weld button that was situated exactly at the bottom of the pipe as shown in Figures 9, 10, and 11. The appearance of this button suggested that it had been placed after completion of the main fillet weld joining the sleeve to the pipe.

The appearance of the remainder of the weld was judged to be relatively rough. The cap pass had been placed using a very wide weave pattern (as compared to the normal stringer pass pattern) and there were a couple of small arc burns in addition to weld spatter adhering to the pipe surface. It is suspected that the original profile of the weld at the top of the pipe had been relatively rough as there was evidence of considerable grinding at this location. Examples of the weld appearance are shown as Figures 12, 13, and 14.

The pipe section was cut so as to open the fracture surface. Examination of this surface prior to any cleaning found a small (30 mm long, 2 mm deep) black coloured feature, likely a pre-existing crack, at the location where the crack was coincident with the heat affected zone of the fillet weld (Figure 15). The fracture surface beneath this feature exhibited a very brittle appearance. Similar brittle fracture was observed on either side of the feature with chevron patterns pointing back to



the position of the black feature, indicating that this was the location of crack initiation (Figures 16 and 17).



FIGURE 3 INITIAL APPEARANCE OF BROKEN PIPE



FIGURE 4 CRACK PATH FROM BOTTOM OF PIPE TO 2:00





FIGURE 5 CRACK PATH FROM BOTTOM OF PIPE TO 10:00



FIGURE 6 EXTENT OF OPENING AT BOTTOM OF PIPE





FIGURE 7 **OFFSET OF FRACTURE AT 9:00**



FIGURE 8 **OFFSET OF FRACTURE AT 3:00**





FIGURE 9 APPEARANCE OF WELD AT BOTTOM OF PIPE



FIGURE 10 WELD "BUTTON" AT BOTTOM





FIGURE 11 WELD "BUTTON"



FIGURE 12 TYPICAL WEAWE PATTERN USED FOR FILLET WELD





FIGURE 13 WELD APPEARANCE AT 4:30

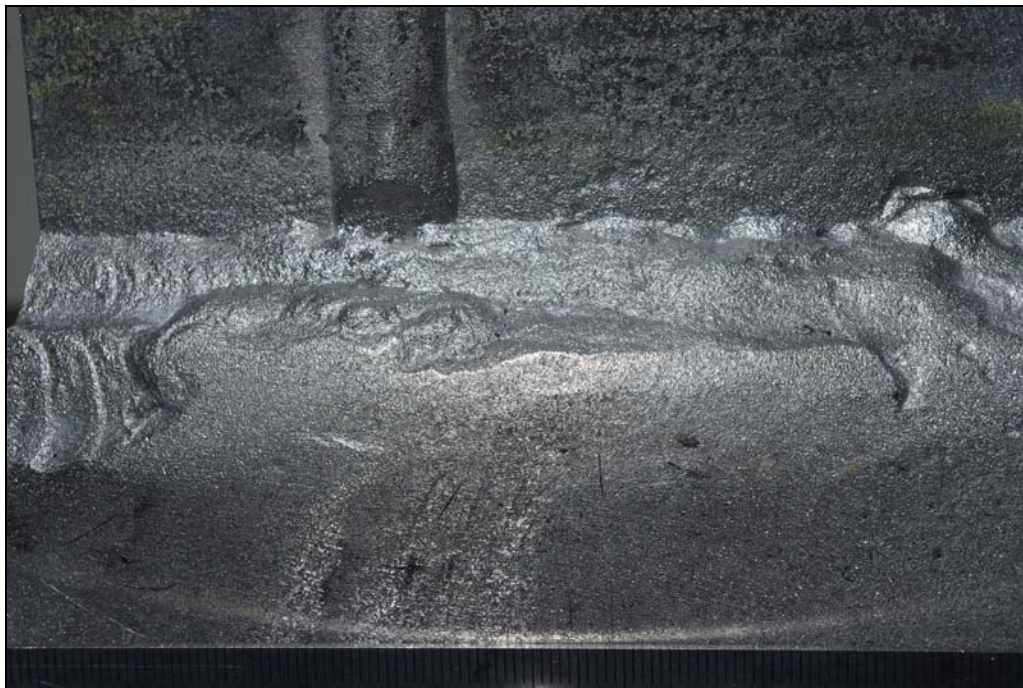


FIGURE 14 WELD APPEARANCE NEAR TOP OF PIPE



FIGURE 15 PRE-EXISTING CRACK AT FRACTURE ORIGIN



FIGURE 16 CHEVRON PATTERN ON BRITTLE CRACK POINTING TO FRACTURE ORIGIN AT PRE-EXISTING FEATURE





FIGURE 17 CHEVRON PATTERN ON BRITTLE CRACK POINTING TO FRACTURE ORIGIN (OPPOSITE SIDE)

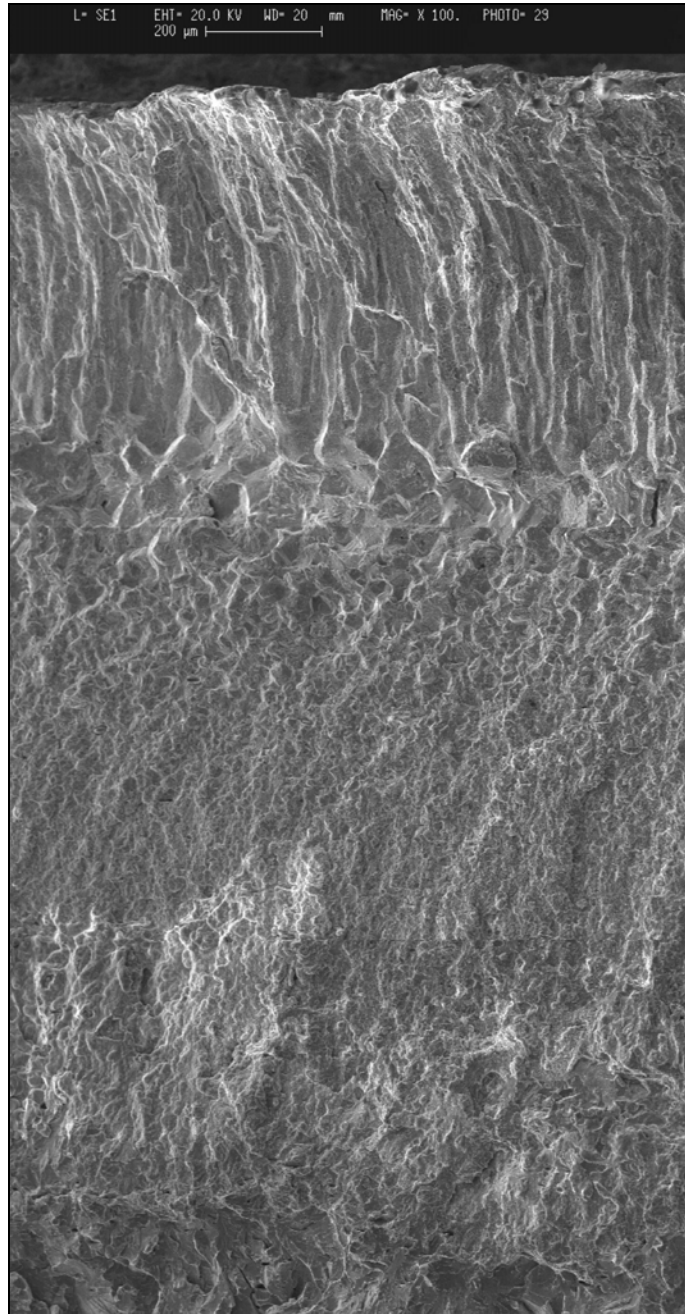
2.2 SCANNING ELECTRON MICROSCOPY

The section of fracture containing the pre-existing flaw was initially cleaned of superficial dirt in a detergent solution and examined in the scanning electron microscope. This instrument is also equipped with an energy dispersive x-ray spectrometer that has the capability of detecting the presence of elements having atomic number 5 (boron) and greater and providing a semiquantitative estimate of the amount of each element detected. This initial inspection found the crack to exhibit a variable appearance (Figure 18) with a columnar structure near the top, an intergranular fracture beneath this and a transgranular appearance for the remainder. The demarcation between the pre-existing crack and the main fracture was clearly seen (as illustrated in Figure 19). A thin layer of scale was apparent on the crack surface to the full extent of the pre-existing crack as shown Figure 20. Energy dispersive x-ray analysis of this scale found it to comprise primarily oxygen and iron as illustrated in the spectrum, Figure 21.

Following this initial inspection, the scale was cleaned from the crack surface using an inhibited acid solution. This cleaning removed the scale uniformly over the entire pre-existing crack very quickly (approximately 30 seconds) as shown in Figure 22, suggesting that the scale was relatively thin over the entire crack. Examination of the sample after cleaning exhibited no indication of any corrosion and clearly showed the intergranular fracture beneath the columnar appearance (Figure 23). Detailed examination of the tip of crack revealed no indication of any progressive crack growth, such as by fatigue. Figure 24 shows the transition from the transgranular pre-existing crack to the final cleavage fracture. This area is shown at higher magnification in Figure 25.

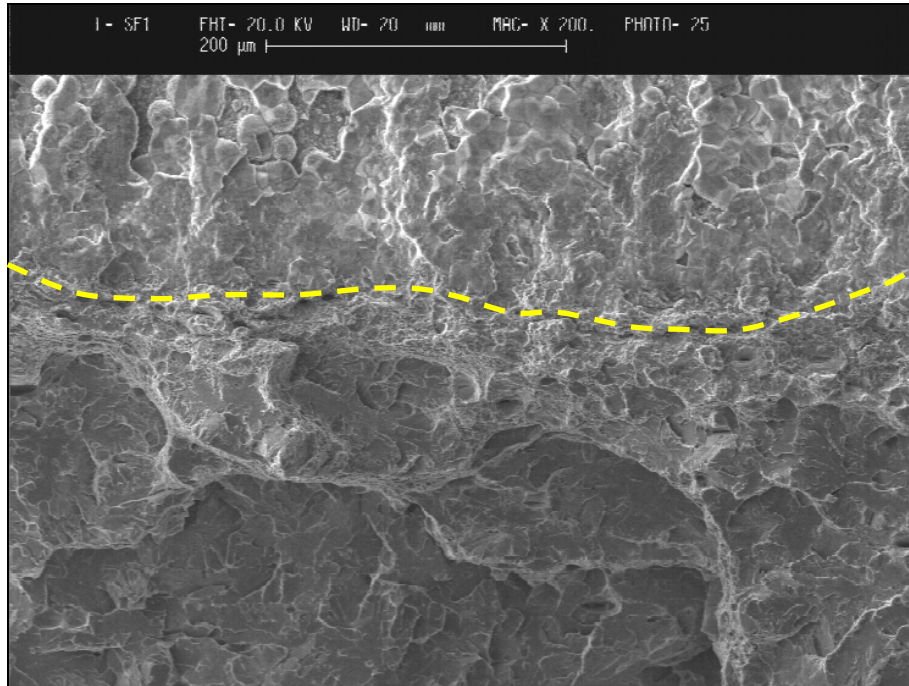
Examination of the rupture surface beyond that of the pre-existing crack found it to be essentially completely brittle cleavage with a small ductile ligament along the inner pipe surface. The general appearance of the fracture at the inner surface is shown in Figure 26. Figure 27 illustrates the brittle cleavage appearance of the majority of the fracture while Figure 28 shows the appearance of the internal ductile ligament.



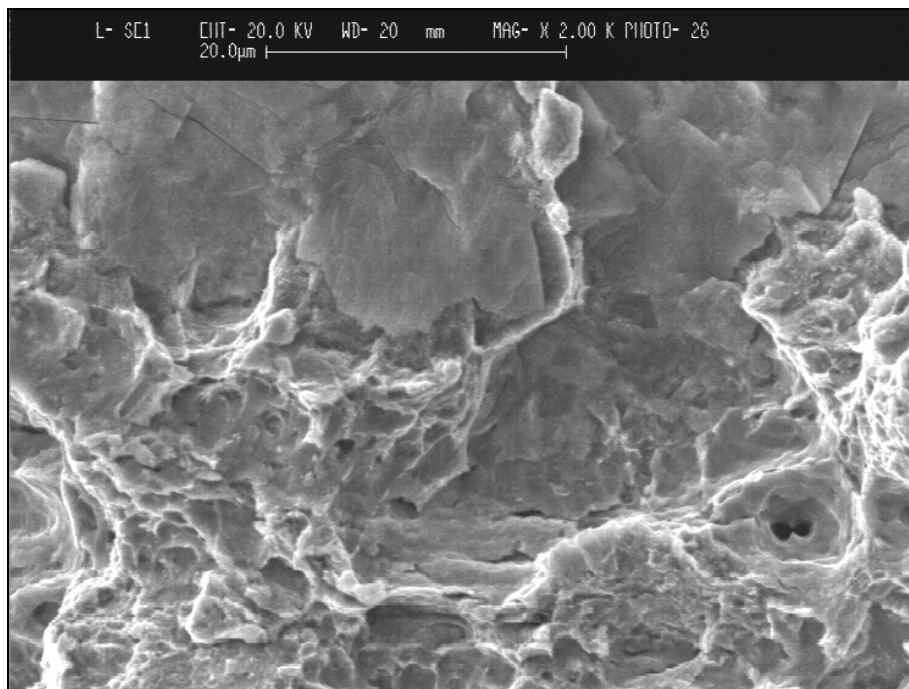


Mag. Approx. X75
FIGURE 18 INITIAL APPEARANCE OF PRE-EXISTING CRACK SURFACE





Mag. Approx. X200
FIGURE 19 CRACK TIP REGION SHOWING EXTENT OF PRE-EXISTING CRACK AND FINAL RUPTURE



Mag. Approx. X2000
FIGURE 20 SCALE TO TIP OF PRE-EXISTING CRACK



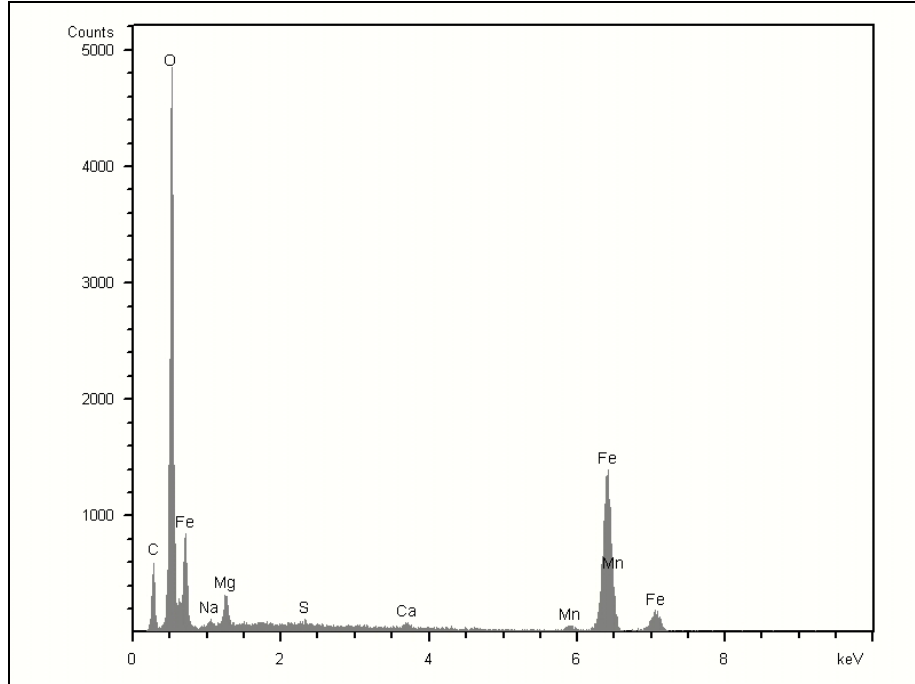
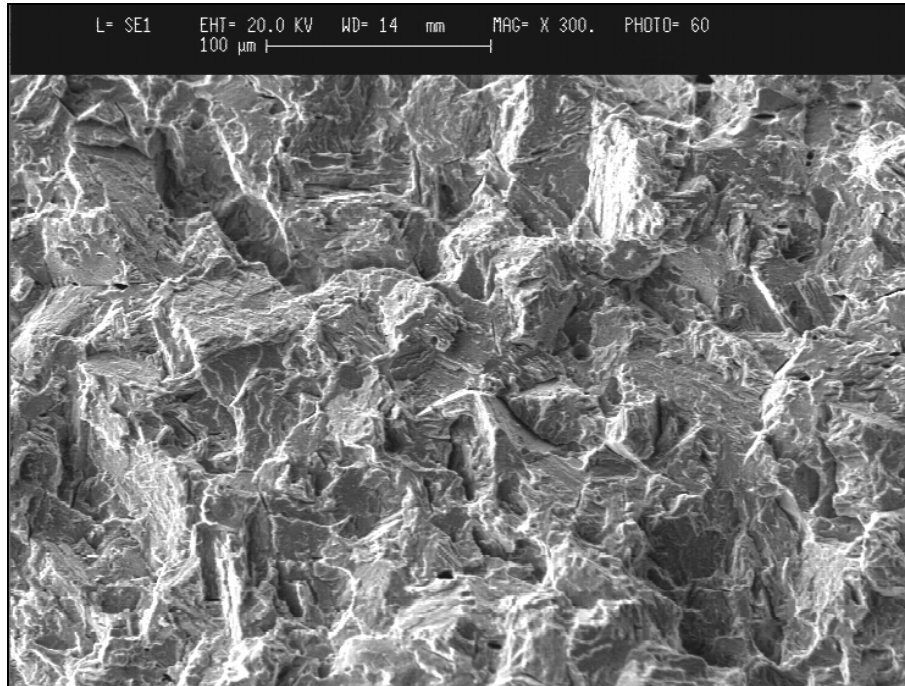


FIGURE 21 EDX SPECTRUM OF SCALE



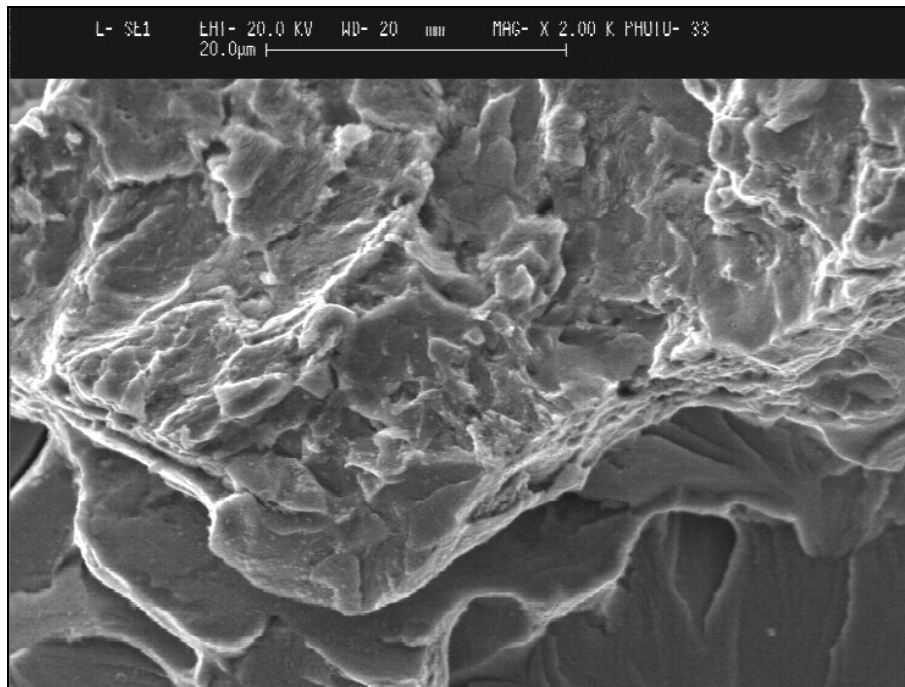
FIGURE 22 PRE-EXISTING CRACK APPEARANCE AFTER 30 SECONDS CLEANING





Mag. Approx. X300

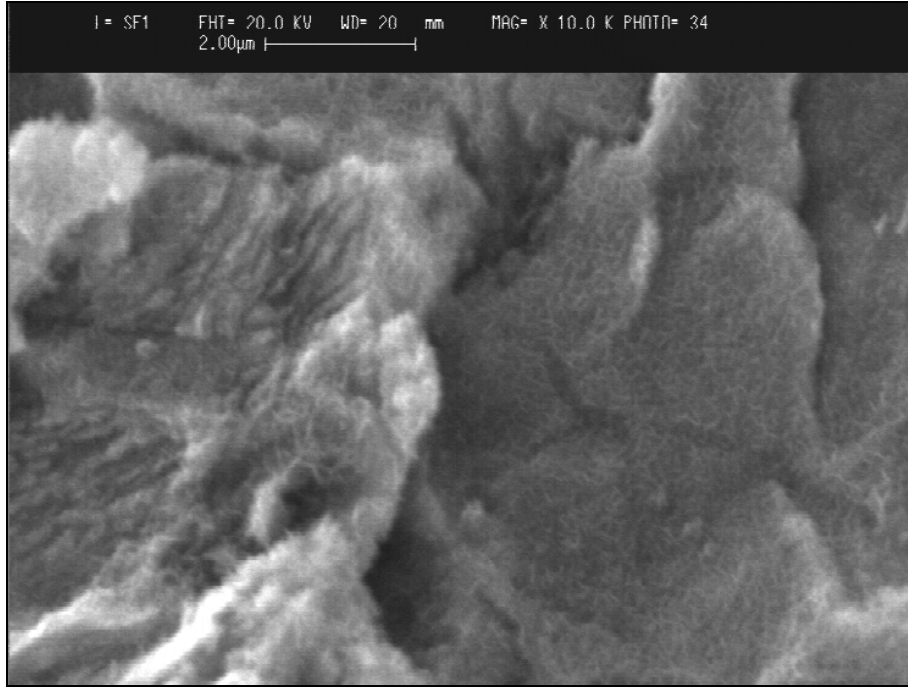
FIGURE 23 INTERGRANULAR CRACKING IN HEAT AFFECTED ZONE



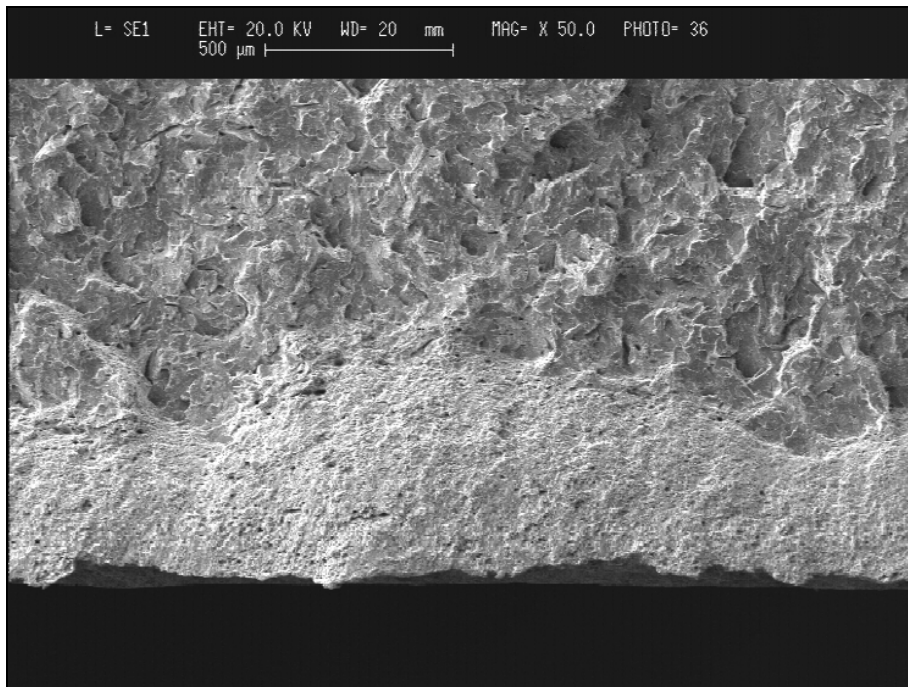
Mag. Approx. X2000

FIGURE 24 CRACK TIP REGION SHOWING ABSENCE OF PROGRESSIVE CRACK GROWTH



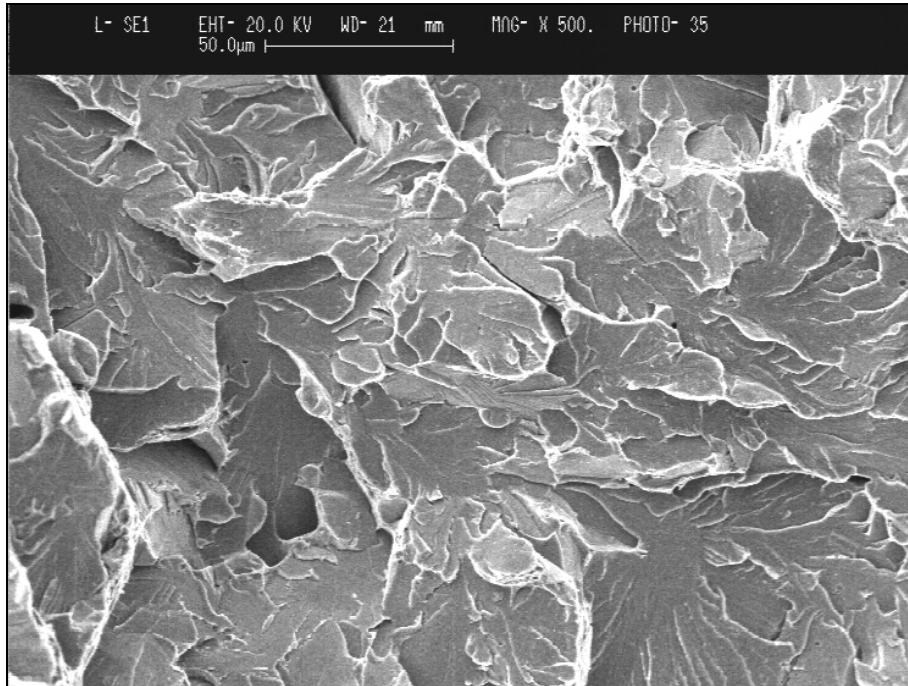


Mag. Approx. X10000
FIGURE 25 CRACK TIP REGION SHOWING ABSENCE OF
PROGRESSIVE CRACK GROWTH

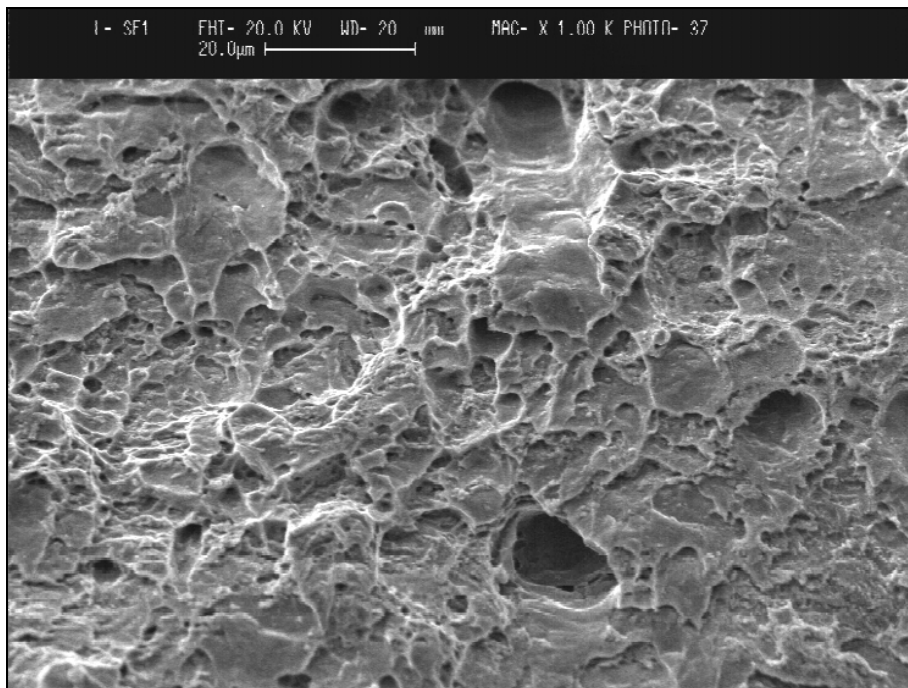


Mag. Approx. X50
FIGURE 26 FRACTURE SURFACE APPEARANCE AT INSIDE OF PIPE





Mag. Approx. X500
FIGURE 27 BRITTLE CLEAVAGE FRACTURE APPEARANCE



Mag. Approx. X1000
FIGURE 28 DUCTILE APPEARANCE OF INSIDE LIGAMENT



2.3 NONDESTRUCTIVE INSPECTION

The fillet weld joining the end of the sleeve to the carrier pipe was examined for evidence of linear indications using wet fluorescent magnetic particle inspection techniques. This inspection found numerous small indications at the toe of the weld on the surface of the carrier pipe as well as at a smaller arc burn. Examples of the indications detected are shown in Figures 29, 30, and 31.

The inspection of the sleeve was repeated using black on white colour contrast magnetic particle inspection to simulate the procedure that would have been used in the field. This inspection detected the same indications that had been found using the wet fluorescent inspection technique. Examples of the appearance of these indications are given in Figures 32 and 33.

Similar inspection on the opposite (upstream) end of the sleeve fillet weld found a 17 mm indication of cracking present at the bottom location (Figure 34), similar to that which was present at the fracture initiation. This indication also appeared to be associated with the edge of the very small weld button (approximately 18 mm long), similar to that present at the fracture initiation site. A number of other very small indications were also detected along the toe of this weld; examples of these indications are shown in Figures 35 and 36.

Inspection of the fillet welds present on the sleeve from Joint 55300 detected a number of small indications along the toe of each weld in addition to an indication associated with an arc burn. Examples of these are shown in Figures 37 and 38.

The fillet weld at the upstream end of the sleeve associated with the failure as well as both welds on the sleeve from Joint 55300 were inspected for indications of cracking at the weld root using an ultrasonic test procedure specifically designed for this type of inspection. This inspection found two small indications on the upstream end of the first sleeve. The first was a spot indication with the ultrasonic signal response (peak height) less than that received from the 0.25 mm notch in the test piece. The second was found to be associated with the linear indication detected at the bottom of the weld and in this case, the response was less than that received from a 0.5 mm notch in the test piece.





FIGURE 29 LINEAR INDICATIONS AT TOE OF FILLET WELD

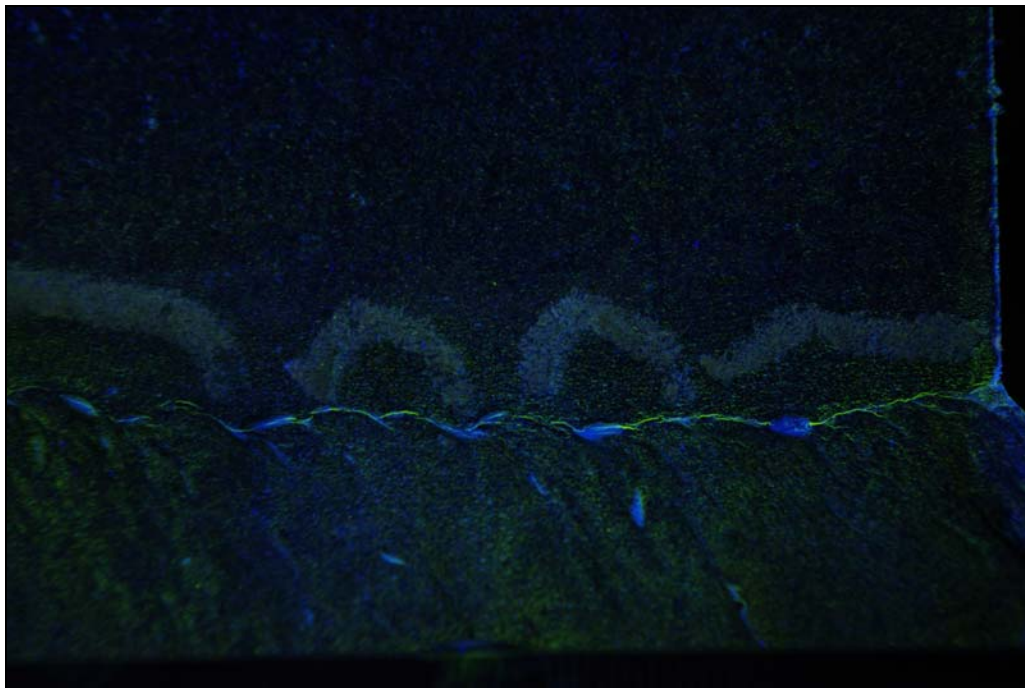


FIGURE 30 LINEAR INDICATIONS AT TOE OF FILLET WELD



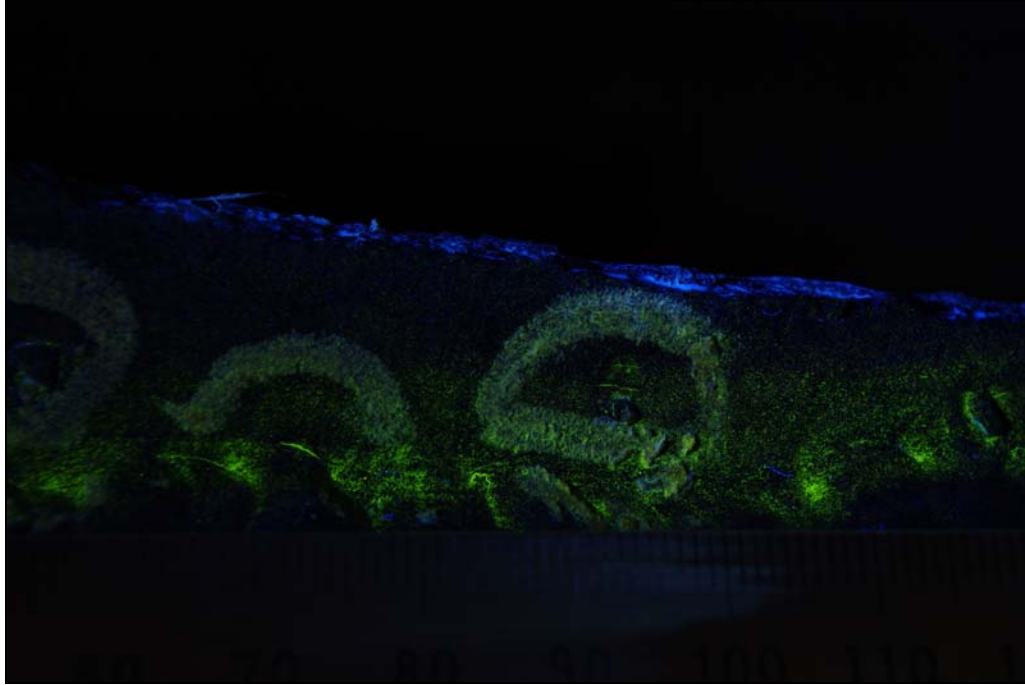


FIGURE 31 LINEAR INDICATIONS AT WELD TOE AND AT ARC BURN



FIGURE 32 LINEAR INDICATIONS DETECTED BY BLACK ON WHITE MPI



FIGURE 33 LINEAR INDICATIONS DETECTED BY BLACK ON WHITE MPI



FIGURE 34 CRACK INDICATION AT BOTTOM OF WELD (UPSTREAM END OF FAILURE SLEEVE)

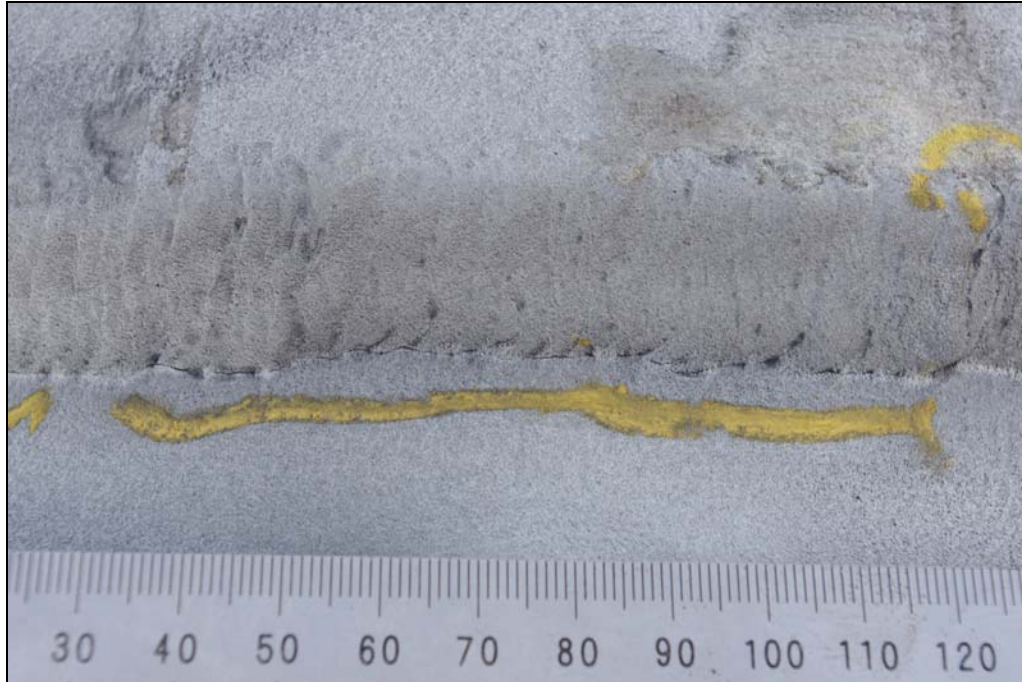


FIGURE 35 CRACK INDICATIONS AT TOE OF WELD
(UPSTREAM END OF FAILURE SLEEVE)



FIGURE 36 CRACK INDICATIONS ADJACENT TO TOE OF WELD
(UPSTREAM END OF FAILURE SLEEVE)



FIGURE 37 INDICATIONS OF CRACKING AT TOE OF FILLET WELD
(SLEEVE ON JOINT 55 300)



FIGURE 38 INDICATIONS OF CRACKING AT ARC BURN ADJACENT
TO FILLET WELD (SLEEVE ON JOINT 55 300)

2.4 METALLOGRAPHY

A matching metallographic section was prepared from the six o'clock orientation of the fracture, in the center of the pre-existing crack. As shown in Figures 39 and 40, failure at this plane had occurred through the edge of the weld and then propagated through the heat affected zone and base material. In the weld, fracture appeared to follow the columnar grain structure (Figure 41). In the heat affected zone, the fracture profile was indicative of intergranular cracking, consistent with that seen on the fracture surface by scanning electron microscopy (see Figure 23). The microstructure of the heat affected zone was noted to be predominantly martensite as shown in Figure 42. The microstructure of the carrier pipe below the heat affected zone was seen to be ferrite and pearlite as shown in Figure 43. This microstructure is considered typical of steel used for line pipe manufactured in the 1960s that did not have any requirements for impact toughness.

The weld profile at the location sectioned was judged to be "reasonable" in that the fillet leg length were comparable although there was some slight underfill at the weld toe on the carrier pipe.

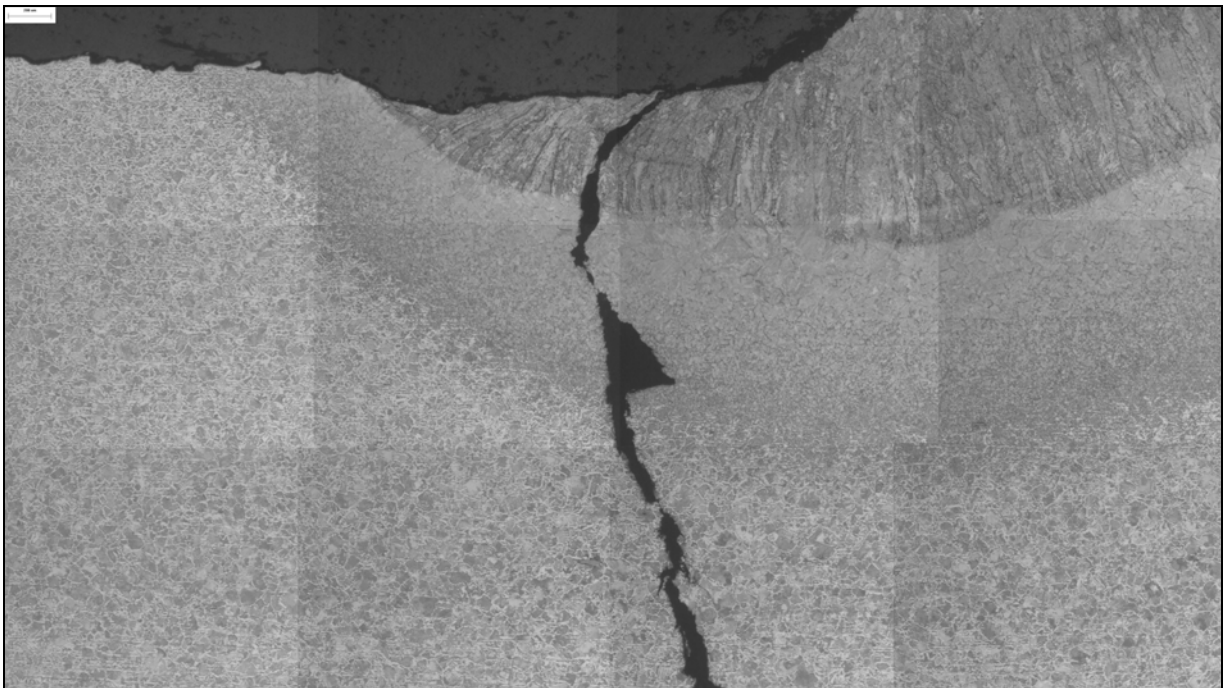
Metallographic sections were prepared from the fillet weld adjacent to the fracture at the top and both sides. The sections are shown in Figures 44, 45 and 46. It is seen that the sections from the top and the two o'clock position exhibited sound welds with good profiles. The section from the ten o'clock position exhibited a reasonably large area of lack of fusion between passes; this area is shown in more detail in Figure 47. This figure also shows a crack generally following the fusion line of the preceding weld pass.

A similar metallographic section was prepared from the location of the magnetic particle indication on the bottom of the upstream fillet weld. This section (Figures 48 and 49) was found to exhibit a very similar (although less deep) crack as that found at the fracture initiation site. The heat affected zone associated with the final weld pass was also seen to be relatively coarse grain martensite as shown in Figure 50.





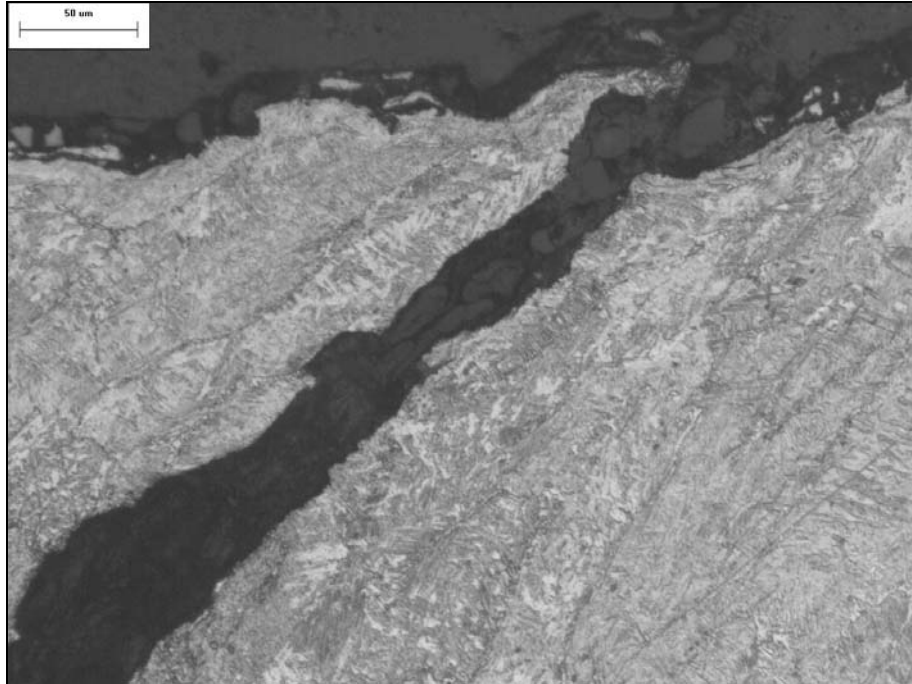
FIGURE 39 METALLOGRAPHIC SECTION FROM 6:00 POSITION



Mag. Approx. X25

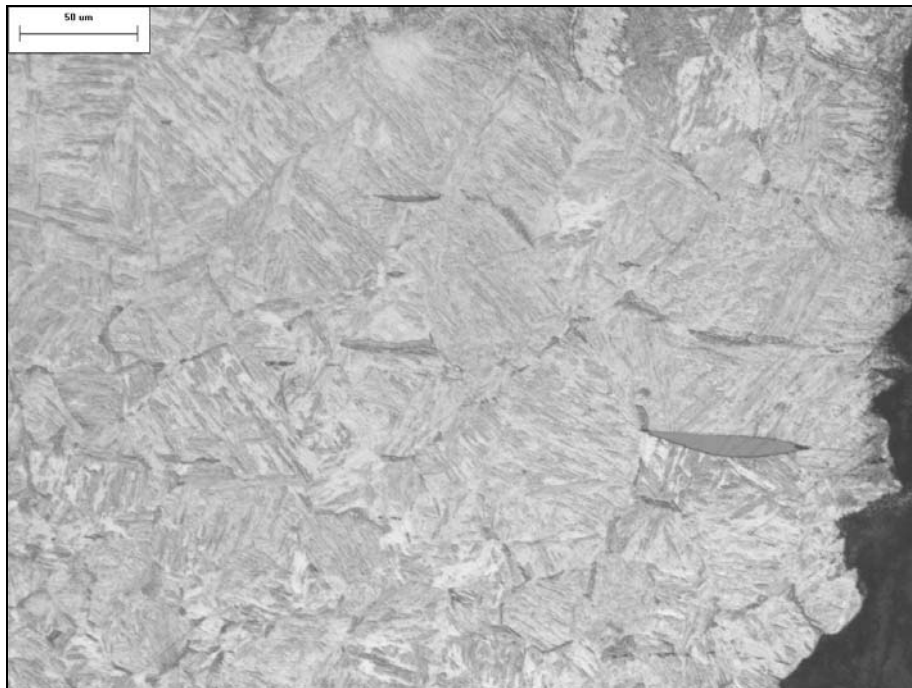
FIGURE 40 CRACK PROFILE AT 6:00 POSITION





Mag. Approx. X300

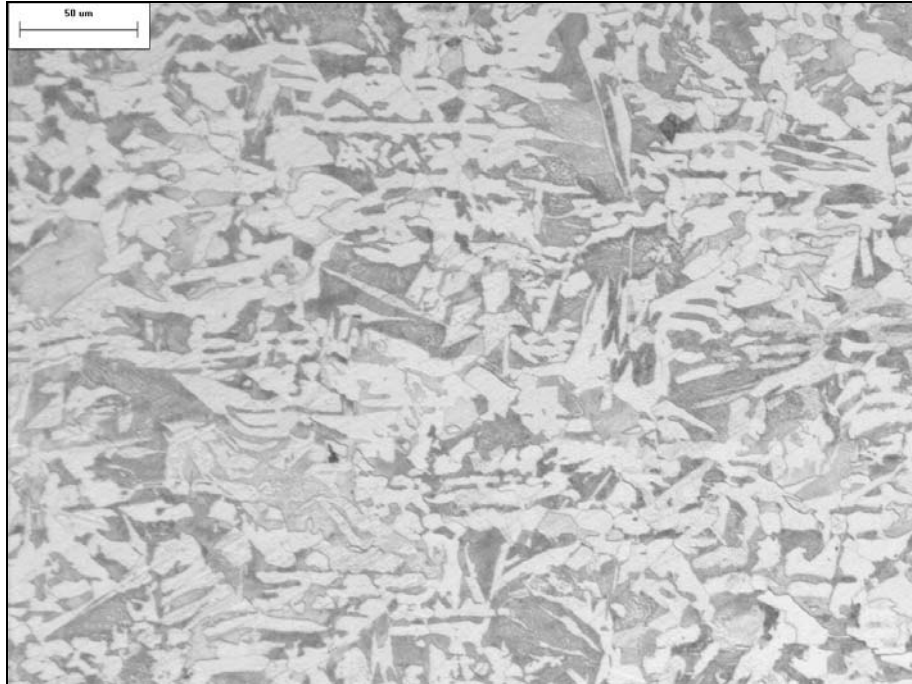
FIGURE 41 FRACTURE PATH THROUGH THE WELD



Mag. Approx. X300

FIGURE 42 MARTENSITIC MICROSTRUCTURE OF HEAT AFFECTED ZONE WITH INTERGRANULAR FRACTURE PATH





Mag. Approx. X300

FIGURE 43 PIPE MICROSTRUCTURE



FIGURE 44 WELD SECTION AT 2:00





FIGURE 45 WELD SECTION AT 10:00

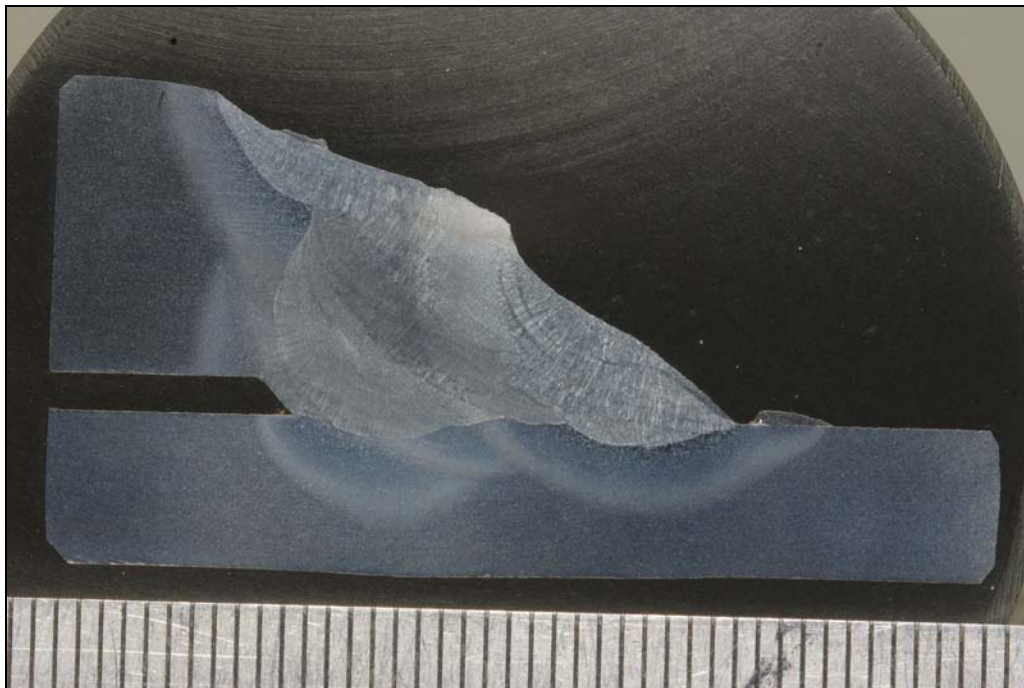
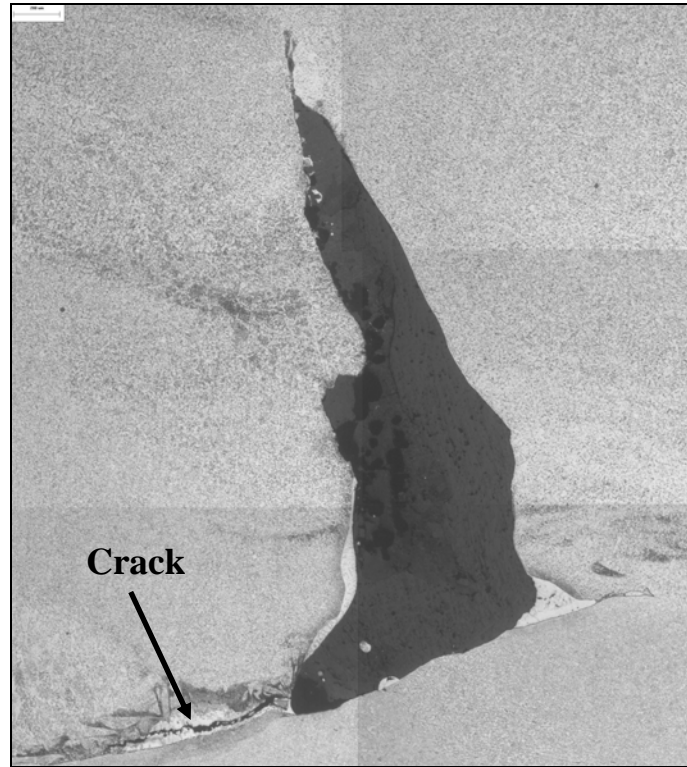


FIGURE 46 WELD SECTION AT TOP



Mag. Approx. X25

FIGURE 47 LACK OF FUSION AT 10:00

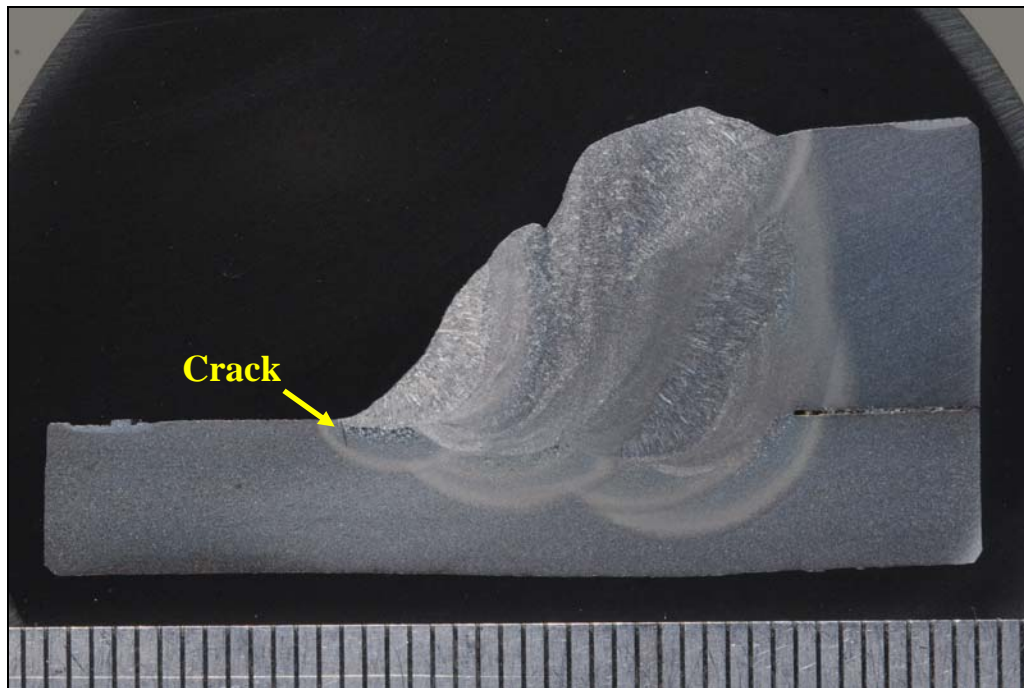
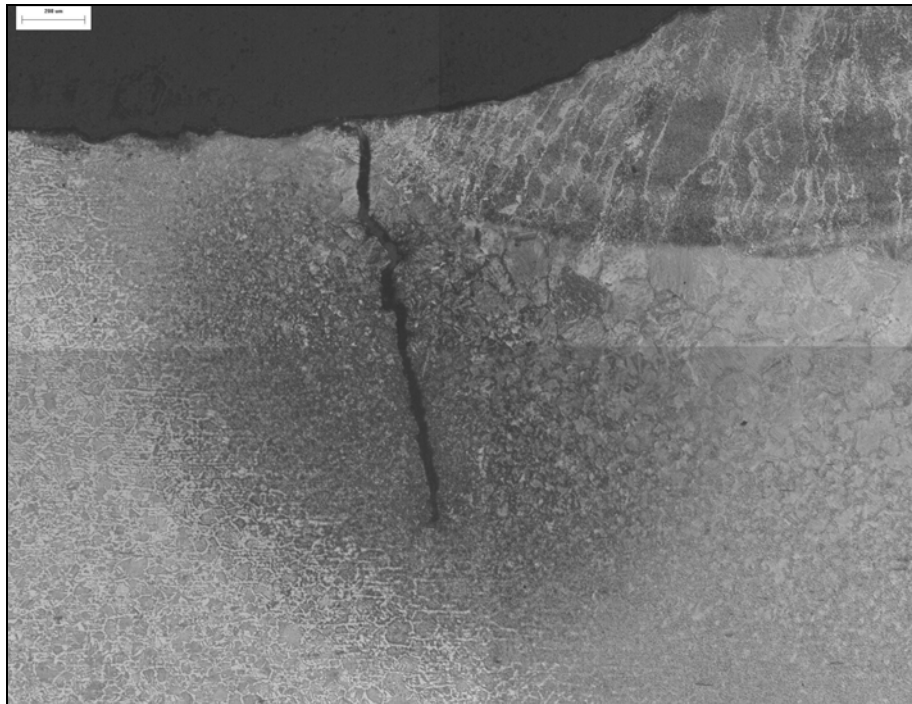


FIGURE 48 SECTION FROM UPSTREAM FILLET WELD AT 6:00





Mag. Approx. X40
FIGURE 49 **CRACK AT TOE OF UPSTREAM FILLET WELD**



Mag. Approx. X300
FIGURE 50 **UPSTREAM HAZ MICROSTRUCTURE**



2.5 MECHANICAL TESTING

2.5.1 Hardness Testing

The hardness of the material in the various zones observed was determined on the prepared metallographic section from the fracture initiation location using a microhardness tester with a 500 gf load. The hardness values obtained on this section are indicated on Figure 51. Hardness values obtained from the outer surface beside the crack through the weld and the heat affected zone associated with the final weld pass from the toe of the weld are shown in Figure 52. The values shown in Figure 51 indicate that the carrier pipe and sleeve have “typical” hardness. The body of the weld is also considered typical while the heat affected zone on the sleeve has slightly elevated hardness values that would still be considered acceptable. In comparison, the hardness values of the final weld pass and those in the heat affected zone beneath this pass are extremely high. It is noted that the current CSA Z662 standard specifies that the heat affected zone hardness shall not exceed 300 HV (compared to the maximum 546 HV measured in this area).

Hardness testing was also performed on the other three sections prepared from the circumference of the weld situated at the fracture. These values are presented in Table 1 and indicate that the hardness values obtained from the two samples from the sides of the pipe were all within an acceptable range. The hardness values in the heat affected zone near the toe of the weld on the carrier pipe were found to be slightly in excess of the specified maximum 300 HV.

Hardness testing of the metallographic section prepared from the 6:00 position on the fillet weld present on the upstream end of the sleeve found the heat affected zone in the vicinity of the crack to again be very hard. Test results obtained from this section are given in Table 2. Further test results beside the crack found on this section found that the hardness ranged from 416 to 460 HV through the weld and from 348 to 257 HV through the heat affected zone.



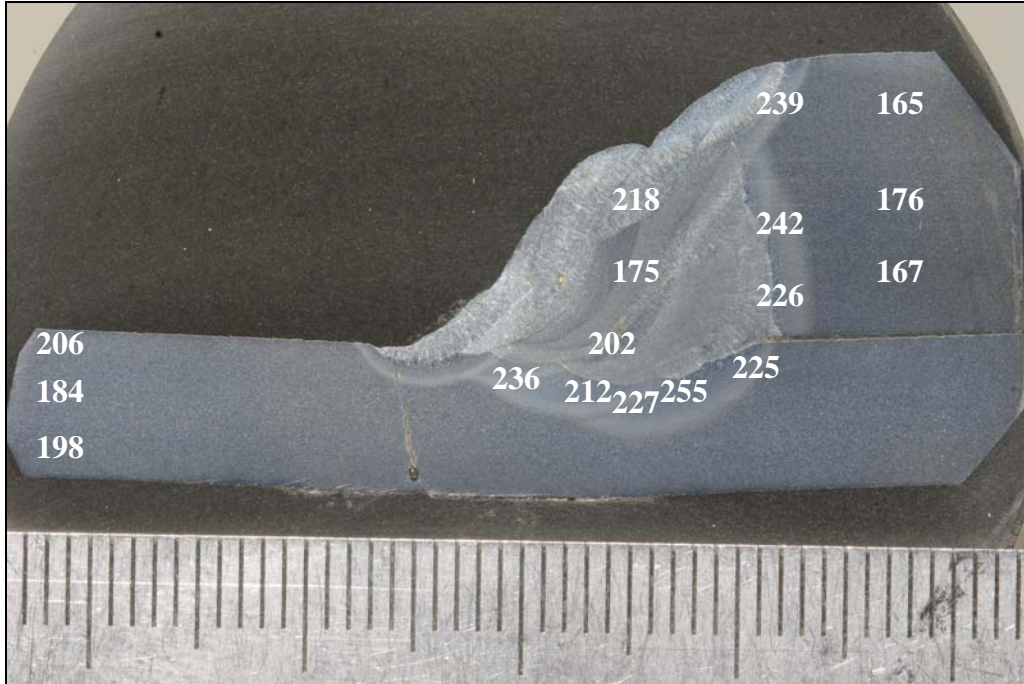


FIGURE 51 HARDNESS VALUES (HV 500gf) AT 6:00

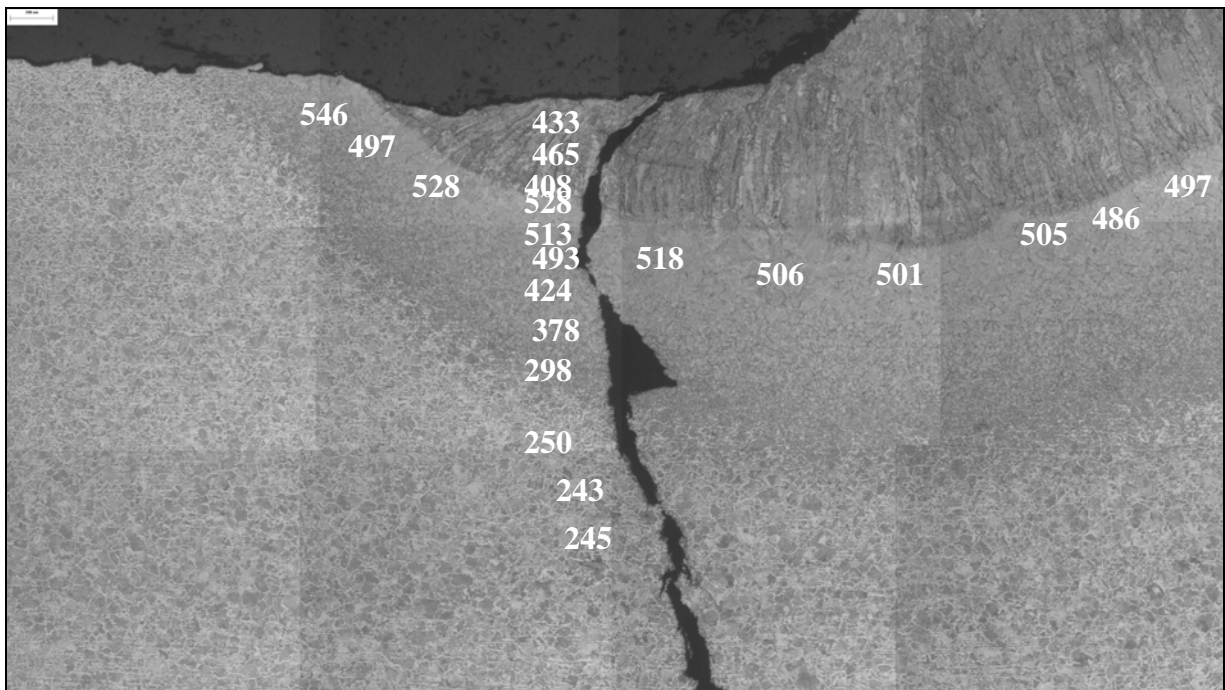


FIGURE 52 HARDNESS VALUES (HV 500gf) NEAR CRACK ORIGIN



TABLE 1 DOWNSTREAM FILLET WELD HARDNESS RESULTS (HV 500gf)

| Location | Pipe Base | Pipe HAZ | Weld | Sleeve HAZ | Sleeve Base |
|-------------|-----------|----------|------|------------|-------------|
| 2:00 | 188 | 230 | 197 | 241 | 180 |
| | 192 | 236 | 180 | 226 | 183 |
| | 184 | 224 | 188 | 227 | 185 |
| | | 184 | | | |
| | | 244 | | | |
| | | 265 | | | |
| 10:00 | 193 | 215 | 219 | 239 | 169 |
| | 189 | 208 | 166 | 217 | 179 |
| | 193 | 206 | 185 | 206 | 173 |
| | | 191 | | | |
| | | 202 | | | |
| | | 190 | | | |
| 12:00 (Top) | 194 | 346 | 236 | 249 | 192 |
| | 185 | 314 | 174 | 264 | 188 |
| | 199 | 316 | 196 | 198 | 200 |
| | | 207 | | | |
| | | 209 | | | |
| | | 180 | | | |

TABLE 2 UPSTREAM FILLET WELD HARDNESS RESULTS (HV 500gf)

| Location | Pipe Base | Pipe HAZ | Weld | Sleeve HAZ | Sleeve Base |
|---------------|-----------|----------|------|------------|-------------|
| 6:00 (Bottom) | 188 | 435 | 203 | 218 | 193 |
| | 206 | 517 | 167 | 215 | 185 |
| | 193 | 461 | 181 | 186 | 194 |
| | | 469 | | | |
| | | 506 | | | |
| | | 238 | | | |
| | | 209 | | | |
| | | 218 | | | |
| | | 232 | | | |
| | | 199 | | | |



2.5.2 Tensile Testing

A transverse flattened strap tensile test coupon was prepared from the body of the ruptured pipe in accordance with requirements of CSA Z245.1 and tested in accordance with ASTM A370. The results obtained from this test are presented Table 3 and indicate that the pipe met the requirements of the specification in place at the time of pipe manufacture (API Standard 5LX, 1967) as well as the current requirements of CSA Z245.1.

A similar test was prepared from the body of the upstream pipe section and has indicated in Table 3, this section also met the requirements of the two specifications.

TABLE 3 TENSILE TEST RESULTS

| | Yield Strength | | Tensile Strength | | Elongation |
|-----------------------|------------------|------------------|------------------|------------------|----------------|
| | MPa | ksi | MPa | ksi | % |
| Pipe Body | 433 | 62.8 | 588 | 85.3 | 29 |
| Transverse Weld | 465* | 67.4* | 609 | 88.4 | 20* |
| Upstream Pipe Body | 418 | 60.6 | 549 | 79.6 | 29 |
| API X52 | | 52.0 Min. | | 72.0 Min. | 20 Min. |
| CSA Grade 359 | 359 - 530 | | 455 - 760 | | 24 Min. |

* - These values are not required by either specifications and are reported for information purposes only



2.5.3 Charpy Impact Testing

One set of longitudinally oriented, 6.4 mm thick Charpy impact specimens was prepared and tested at +5° C (the estimated temperature of the line at the time of failure). This thickness was chosen as it was the maximum obtainable from the pipe and so would best represent the actual toughness of the material. The results obtained from this test are present in Table 4.

Six sets of transversely oriented Charpy impact specimens were also prepared and tested at various temperatures to determine the transition behaviour of the steel. Test temperatures included -5° C, as this is the normal qualification temperature for buried pipe manufactured to the current CSA Z245.1, Category II requirements. The samples had a thickness of 5.9 mm. The results obtained from this series of tests are presented in Table 5, and are shown graphically in Figure 53. This table also includes the average full size equivalent (FSE) absorbed energy values as calculated by the procedures given in API 579-1, Annex F4.3.2 d. It is seen that the 50% shear area transition temperature of this steel is approximately 24° C. Similar transverse samples were prepared from the upstream section of the pipe received and as included in Table 5, the results were seen to be almost identical to those obtained from the ruptured pipe (as a full curve was not developed for this pipe, the full size equivalent values were not calculated).

TABLE 4 CHARPY IMPACT TEST RESULTS – LONGITUDINAL SAMPLES

| | Pipe Body – Longitudinal Samples | |
|------------------|---|-----------------------|
| Test Temp | Absorbed Energy | Shear Fracture |
| °C | J | % |
| +5 | 34 | 40 |
| | 30 | 30 |
| | 45 | 50 |
| Average | 36.3 | 40.0 |



TABLE 5 CHARPY IMPACT TEST RESULTS – TRANSVERSE SAMPLES

| Test Temp °C | Failed Pipe Body | | | Upstream Pipe Body | | |
|-----------------|----------------------|-----------------------|---------------------|----------------------|--|---------------------|
| | Absorbed Energy J | Full Size Equiv. J | Shear Fracture % | Absorbed Energy J | | Shear Fracture % |
| | J | J | % | J | | % |
| -20 | 7 | 7.2 | 5 | | | |
| | 14 | | 10 | | | |
| | 12 | | 10 | | | |
| Average | 11.0 | | 8.3 | | | |
| -5 | 16 | 8.9 | 20 | | | |
| | 14 | | 10 | | | |
| | 9 | | 5 | | | |
| Average | 13.0 | | 11.7 | | | |
| 10 | 17 | 12.4 | 30 | 16 | | 20 |
| | 15 | | 30 | 18 | | 20 |
| | 17 | | 30 | 15 | | 20 |
| Average | 16.3 | | 30.0 | 16.3 | | 20.0 |
| 25 | 18 | 19.2 | 50 | 21 | | 50 |
| | 20 | | 50 | 20 | | 50 |
| | 23 | | 50 | 22 | | 50 |
| Average | 20.3 | | 50.0 | 21.0 | | 50.0 |
| 40 | 20 | 29.4 | 60 | 31 | | 80 |
| | 25 | | 70 | 24 | | 60 |
| | 24 | | 70 | 27 | | 60 |
| Average | 23.0 | | 66.7 | 27.3 | | 66.7 |
| 55 | 34 | 40.7 | 100 | | | |
| | 34 | | 100 | | | |
| | 34 | | 100 | | | |
| Average | 34.0 | | 100.0 | | | |



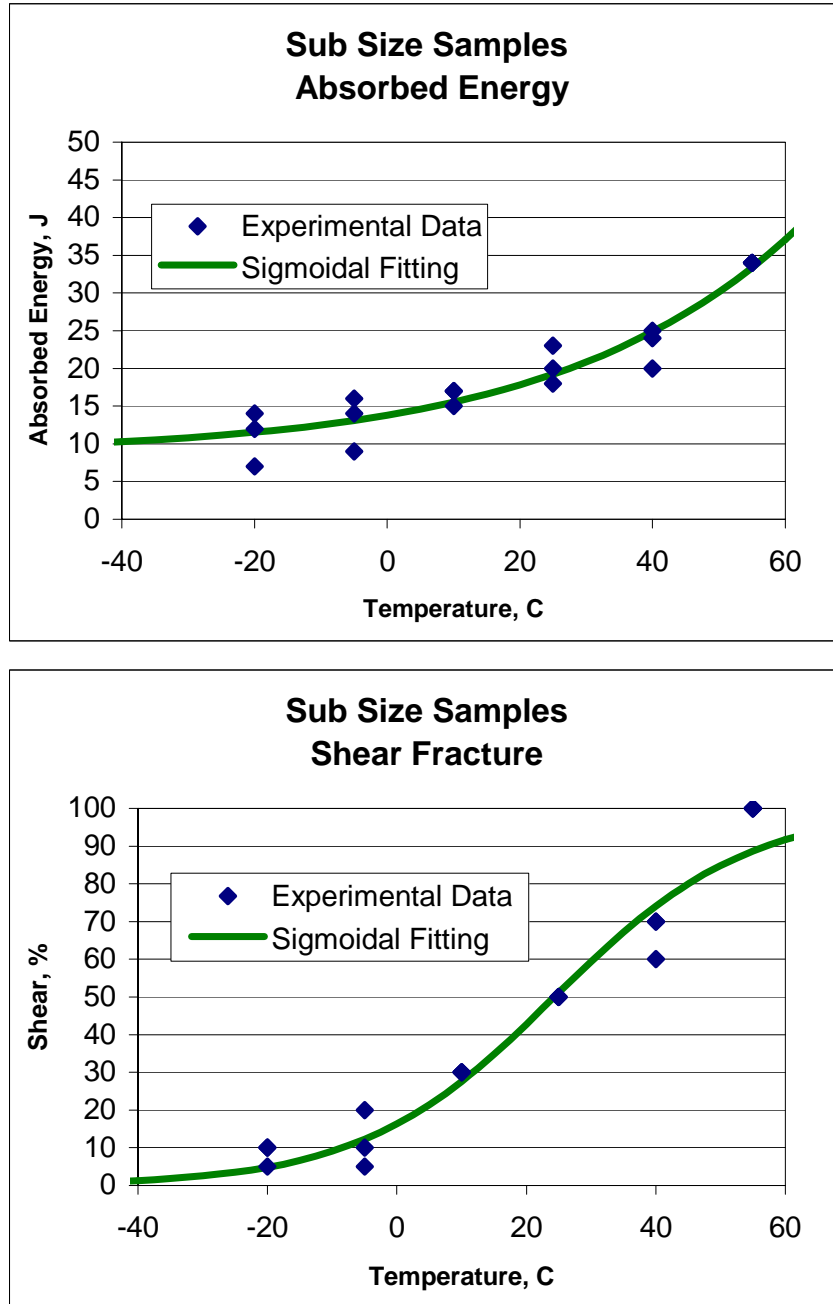


FIGURE 53 CHARPY TRANSITION CURVES



2.6 CHEMICAL ANALYSIS

The chemical composition of the failed carrier pipe was determined using an inductively coupled plasma spectrometer in conjunction with a Leco carbon/sulfur analyzer. The results are presented in Table 6 and show that the carbon content of the pipe exceeded the ladle analysis limit of the specification in place at the time of pipe manufacturer (API 5LX-X52 – 1967) but was within the tolerance allowed for product analysis. The carbon content does exceed the current maximum allowed by CSA Z245.1 – 07 as does the calculated carbon equivalent.

TABLE 6 CHEMICAL TEST RESULTS

| Element | Rupture | API 5LX-X52 | CSA Z245.1 |
|--------------------|----------------|--------------------|-------------------|
| Carbon | 0.31 | 0.28 Max.** | 0.26 Max. |
| Manganese | 1.18 | 1.25 Max. | 2.00 Max. |
| Phosphorus | <0.010 | 0.04 Max. | 0.030 Max. |
| Sulphur | 0.018 | 0.05 Max. | 0.035 Max. |
| Silicon | 0.040 | N.S. | 0.50 Max. |
| Nickel | 0.022 | N.S. | N.S. |
| Chromium | 0.034 | N.S. | N.S. |
| Molybdenum | <0.010 | N.S. | N.S. |
| Copper | 0.015 | N.S. | N.S. |
| Vanadium | <0.010 | N.S. | 0.11 Max. |
| Niobium | <0.010 | N.S. | 0.11 Max. |
| Titanium | <0.010 | N.S. | 0.11 Max. |
| Aluminium | <0.010 | N.S. | N.S. |
| Boron | <0.0003 | N.S. | 0.001 Max. |
| Cobalt | <0.010 | N.S. | N.S. |
| Tungsten | <0.010 | N.S. | N.S. |
| Arsenic | <0.010 | N.S. | N.S. |
| Tin | <0.010 | N.S. | N.S. |
| Carbon Equivalent* | 0.53 | N.S. | 0.40 Max * |

N.S. = Not Specified; All values expressed as weight %.

* Carbon equivalent calculated in accordance with CSA Z245.1

** API 5LX permits the C check analysis to exceed the ladle analysis limit by +0.04%



3.0 DISCUSSION

Examination of the section of failed pipe from the Rainbow Pipeline has found that the pipe fractured in a brittle manner, with the fracture initiating at the location of a small pre-existing crack at the toe of a fillet weld joining a sleeve to the pipe body. It is our opinion that the crack formed very soon after completion of the fillet weld and remained dormant until such time as the longitudinal stress on the crack reached some critical value. Once this stress was achieved, the pipe fractured in a one time catastrophic event. No indication was found to suggest that there had been any leak that preceded the failure. Details of our findings leading to this conclusion are as follows.

Examination of the fracture surface found a scale covered semi elliptical shape crack extending from the outer surface of the pipe at the six o'clock orientation. Chevron markings on the brittle fracture on the remainder of the crack clearly showed that this pre-existing crack had acted as the fracture initiation point.

The initiating crack had a total length of approximately 30 mm with a maximum depth of 2.0 mm. This feature was covered with a black iron oxide scale that was readily and uniformly removed with inhibited acid. These features, in combination with the absence of any significant corrosion on the crack face (as observed by subsequent scanning electron microscopic examination), indicate that the crack had formed as a one-time event and was not the result of stress corrosion cracking. It is suspected that the scale on the crack surface formed while the surrounding material was still very hot at the completion of welding. Subsequently, the presence of coating over the weld prevented any corrosion.

Examination of the fracture surface appearance of the initiating crack as well as the microstructure and hardness in the immediate vicinity of the crack found the crack had followed the columnar grain structure of the weld and then progressed as an intergranular crack through the coarse grain heat affected zone. The crack then followed a transgranular pattern through the remainder of the heat affected zone where it arrested. The weld and the coarse grain heat affected zone beneath the weld were found to be extremely hard and, consequently, very brittle. This high hardness is consistent with the observed intergranular crack path. The stress responsible for the formation of the crack at this time would have occurred as a result of thermal contraction of the hot weld and surrounding material.

Nondestructive inspection of the fillet weld on the upstream end of the sleeve associated with the rupture found a similar crack present at the six o'clock orientation. This crack was also associated with a very coarse grain heat affected zone, very similar to that found at the fracture initiation site.



Another common feature of the two fillet welds was the presence of a very small weld button at the six o'clock orientation. It was only immediately beneath these small weld buttons that the hardness of the heat affected zone was very high. Hardness values as high as 546 HV were measured nearer these buttons whereas the maximum hardness at other locations was only 346 HV (measured at the toe of the fillet weld at the top location). It is suspected that the same welder probably placed both fillet welds on the sleeve. He probably observed some visual feature at the six o'clock position of both welds and decided to "fix" these features by applying the very small weld buttons. As this probably occurred after the welds had cooled and he did not follow the prescribed weld procedure, these very small welds cooled very rapidly, resulting in the generation of the high hardness values. The other locations tested on the fillet welds were found to exhibit reasonable, although slightly excessive, hardness values. This suggests that had the prescribed weld procedure been followed at all times, the very high hardness regions would not have been present. In the absence of such high hardness regions, the probability of cracking at the toe of the weld would have been extremely low.

The carbon equivalent of the carrier pipe at the location of the cracking was found to be very high as a result of the high carbon content. The carbon equivalent would increase the hardenability of the steel, such that martensite would form more readily on cooling from welding temperatures. The carbon content would increase the hardness of any martensite that did form (since the hardness of martensite is directly related to the carbon content). However, the absence of any excessive hardness at locations other than in the vicinity of the small weld buttons present at the bottom of both upstream and downstream fillet weld on the sleeve indicates that the welding procedure used to attach the sleeve was generally satisfactory.

As noted above, it is our opinion that the crack formed immediately after placement of the small weld buttons. No evidence was found to indicate that the crack had grown at all as a result of fatigue since its initial formation and the failure event. Rather, it is thought that the crack remained stagnant until the longitudinal stress present at the bottom of the pipe reached a critical value. Once this occurred, rapid brittle fracture ensued. The amount of opening at the bottom of the pipe with the fracture running up either side indicates that the stress at the bottom of the pipe resulted from a sag in the pipe. The slight offset observed on the pipe sides further indicates that there was a very small torsional stress on the pipe. No evidence was found to suggest that the pipe had leaked prior to the fracture event.

The longitudinal stress responsible for the fracture would have been the result of an unsupported sag in the pipe at the location of failure. It is thought likely that this sag developed over the life of the pipe, or at least since the placement of the sleeve in 1980. No information was available regarding details of how much pipe was exposed during this operation or what, if any, support was placed under the pipe during the sleeve installation. Similarly, the effectiveness of compaction of the backfill under the pipe was not known. Consequently, it is possible that some sagging may



have occurred at this time. It was also reported that the sleeve had been exposed for inspection in 1989/1990. Again, it was not known how much pipe was inspected or any other details to suggest that there might have been some contribution to the amount of sagging at this time. The failed section of pipe had been exposed for a third time in 2010 when it was thought that approximately 7 m of pipe had been uncovered. The possibility of inadequate compaction of the soil under the pipe during backfilling could again have contributed to the degree of sag and therefore the longitudinal stress. The total stress at the position of failure was still not sufficient to cause failure at this time. However, it is suspected that thawing of the soil around the pipe this spring and the associated movement associated with this further contributed to this stress to the extent that it was high enough to result in failure.

As the longitudinal bending stress increased in the pipe, the stress intensity at the tip of the pre-existing crack also increased. Once this stress intensity reached a critical value (termed K_{IC}), brittle fracture occurred. The longitudinal stress required to reach this critical stress intensity value would have been significantly less than that required for ductile failure of the pipe.

The value of K_{IC} is a material property that is related to the Charpy impact toughness. Charpy testing of the ruptured pipe found the material to exhibit the generally poor toughness at the temperature at which rupture occurred. Consequently, the K_{IC} of the pipe would also be anticipated to be very low. This finding is consistent with the very brittle nature of the fracture extending from the initiation point. The brittle characteristics of the pipe resulted in a one time catastrophic failure event.

It has been proposed that the crack formed immediately after welding and was present from then until the time of failure. It is assumed that the weld would have been inspected for evidence of cracking prior to backfilling the pipe. This implies that the inspection did not find this crack. It is noted that the crack was situated at the bottom of the pipe and would therefore have been at a location where crack indication could be missed. Firstly, it is an awkward position to view closely and secondly, the particles present in the wet suspension used during magnetic particle inspection would tend to run to the bottom of the pipe and so a collection of particles might be incorrectly assumed to be simply this collection rather than the result of a crack. However, it was also noted that there were a number of small linear indications detected at other locations around the toe of the weld and these had obviously been accepted. A similar argument could be made for the inspection that had been performed in 1989/1990. It was reported that the weld was not uncovered and inspected during the 2010 dig.

Mechanical testing of the carrier pipe found that it met the requirements for Grade 359 (X52) of both the API specification in place at the time of pipe manufacture as well as the current CSA Z245.1 specification. As noted above, the Charpy impact toughness of the pipe was considered to be poor and would not meet the current CSA S448.1 requirement for Category II pipe. It is



realized that the pipe would not have required proven impact toughness when it was installed and consequently this does not indicate that the pipe did not meet the requirements of the specification. It was noted that the results of the longitudinal Charpy test were considerably better than those of the transverse samples. It is suspected that this could be related to the and direction of plate rolling at the time of steel manufacture.



4.0 CONCLUSIONS

It is our opinion that failure of the Rainbow Pipeline occurred as a result of the combination of:

- Failure to follow the prescribed weld procedure during welding of the sleeve to the carrier pipe.
- A very high carbon equivalent of the carrier pipe.
- Failure to detect a small crack during two separate inspections of the weld attaching the sleeve to the pipe.
- The development of a sufficient bending stress in the pipe as a result of local sagging of the pipe.
- The poor toughness of the pipe that resulted in a wide open brittle fracture.

Prepared By,



E.C. (Ted) Hamre, Ph.D., P. Eng.
Engineering Technical Leader

Reviewed By,
Ken Magee, M.A.Sc., P. Eng.
Senior Metallurgical Engineer

APEGGA Permit Number: P5386 (Alberta)

CB2011-206-0059227_01-01R0 Rainbow Failure.doc

Please note that unless we are notified in writing, samples from this investigation will be disposed of after 60 days.

